J Mater Sci (2016) 51:2181–2198
DOI 10.1007/s10853-015-9503-1

REVIEW

Recent progress of synthesis and applications in polyoxometalate and nanogold hybrid materials

Umsa Jameel[1] · Mingqiao Zhu[1] · Xinzhi Chen[1] · Zhangfa Tong[2]

Received: 3 June 2015 / Accepted: 13 October 2015 / Published online: 23 October 2015

Abstract The role of polyoxometalates (POMs) in the synthesis and stabilization of gold nanoparticles (Au NPs) is reviewed in light of many of the recent developments. The vitality of these hybrid materials is discussed with many examples of POMs and different synthesis techniques. Also, applications of these newly emerging hybrid materials in numerous fields such as electrocatalysis, photocatalysis, biomass catalysis, oxidation of alkenes, bio-sensing, and medicinal use are highlighted. Limitations in these applications are indicated, and areas of future applications that could be explored in these vast ranging hybrid materials are described.

Introduction

In recent years, the study of nanoparticles (NPs) has been a vast area of research owing to size-dependent chemical and physical properties that allow tuning of NP properties. Techniques for the synthesis of nanomaterials with a preset size, shape, and chemistry are the focus of many research groups. Metal NPs possess many interesting spectroscopic, electronic, optical, magnetic, catalytic, and chemical characteristics that result from their small size and high surface/volume ratio [1]. In addition, the control of NP size and composition influences electronic structure and catalytic properties [2–5].

NPs are prepared through self-assembly into ordered and stable organizations mediated by surfactants, ligands, and other factors that are not always intuitive but are critical to reproducibility. Different hydrophobic compounds like alkylamines, alkanethiols, and cationic surfactants have been employed to induce NPs toward self-organization [6], and different geometrical forms of gold nanoparticles (Au NPs) have been synthesized [7–9] that have broad applications for devices such as optical gratings, antireflective surface coatings, sensing, biodiagnostics, surface-enhanced Raman spectroscopy, and DNA detection [6, 10, 11].

The different forms of Au NPs are acknowledged as effective catalysts for industrially vital reactions including oxidations and hydrogenations [12, 13] and also many biological and biomedical applications [14]. The capability of Au NPs as oxidation catalysts highly depends upon size with smaller NPs as better catalysts. This observation makes the inhibition of sintering or aggregation of NPs an important objective, and much work has been devoted to NP supports as well as the support's influence on activity and recyclability [15–20]. Polyoxometalates (POMs) possess high potential as supports for NPs [21] as their high anionic charge appears to enhance stability, as well as avoiding sintering of the NPs [22, 23]. However, there is little research regarding the mechanism for anions (especially POMs) in stabilizing and tuning the properties of Au NPs.

POMs comprise a large class of metal–oxygen anions including group V and VI transition metals [24]. The more common transition metal ions forming the molecular structural framework of POMs are W (VI), Mo (VI), V (V), Nb (V), Ta(V), and Ti(IV) [25]. These ions or their local

✉ Mingqiao Zhu
zhumingqiao@zju.edu.cn

[1] Key Laboratory of Biomass Chemical Engineering of Ministry of Education, College of Chemical and Biological Engineering, Zhejiang University, Hangzhou 310027, China

[2] Guangxi Key Laboratory of Petrochemical Resource Processing and Process Intensification Technology, School of Chemistry and Chemical Engineering, Guangxi University, Nanning 530004, China

MO_x coordination polyhedra are called addenda ions. The structures contain MO_6 octahedra most commonly, but in some cases MO_5 pentahedral and MO_4 tetrahedral elements also exist. Most studies among all structures are regarding the Keggin heteropolyanions of formula $[X^{n+}M_{12}O_{40}]^{(8-n)-}$, where M = W (VI) or Mo (V1). The heteroatom, X^{n+}, can be one of the p-block elements [26].

These complexes are readily prepared, well characterized, and stable. POMs are negatively charged although the negative charge density is extensively variable, depending upon the structure and elemental composition [26]. The variety of size, topology, elemental composition, and electronic properties of POMs provides many avenues for research into their chemistry [27], exploring potential applications in areas such as functional materials with applications in separation, catalysis, ion exchange, sorption, electrochromism, electrochemistry, magnetic and supramolecular chemistry, materials science, and medicine [24, 27–31].

The role of POMs in the support and stabilization of NPs is a recent development in this field. The anionic charge provides electrostatic repulsion between the POMs thus preventing the agglomeration of supported Au NPs [32]. These characteristics of POMs make them powerful in the synthesis of metal NPs using simple, efficient, and ambient-temperature techniques [33] providing a new class of stabilizers better than conventional organic stabilizers. The pH-dependent stability of POMs allows control, with a change of pH to remove the NPs unlike the organic ones [34]. More recently, research has been dedicated to the fabrication of a wide variety of POMs and NPs such as carbon nanotubes [35], Pt NPs [36], Fe_3O_4 NPs [37], TiO_2 NPs [38], Bi_2O_3 NPs [39], and Ag NPs [40] to explore synergistic properties arising from POM-supported NPs. This micro-review is based on recent developments in POM-supported Au NP hybrid materials focusing on the synthesis of POM-supported Au NPs and applications ranging from bifunctional catalysis, optics, and magnetics to environmental engineering and medicine.

Syntheses of POM–gold nanoparticle hybrid materials

POMs as capping and stabilizing agents for Au NPs

Finke demonstrated the use of POMs as stabilizers for iridium and rhodium nanoclusters with the niobium-containing POMs $[P_2W_{15}Nb_3O_{62}]_9^-$ and $[SiW_9Nb_3O_{40}]_7^-$ with tetraalkylammonium counter ions [41, 42]. Finke and Özkar presented a study of different anionic stabilizers and suggested five criteria for stabilizer providing the first ''anion series'' ($P_2W_{15}Nb_3O_{62}{}^{9-}$ ~ $SiW_9Nb_3O^{407-}$>$C_6H_5O_7{}^{3-}$ ~ $-[CH_2CH(CO_2^-)-]_n$ $^{n-}$ ~ OAc^- ~ $P_3O_9{}^{3-}$ ~ Cl^- ~ OH^-) [43]. They proposed the coordination of anionic stabilizers to the nanoclusters via trigonal facial oxygen of a metal octahedron. Their studies rank $[P_2W_{15}Nb_3O_{62}]^{9-}$ as the best stabilizer for Ir^0 nanoclusters in part due to lattice size matching [44]. Pre-functionalized POM γ-$[SiW_{10}O_{36}(RSi)_2O]^{4-}$ was used by Mayer et al. [45] during Au NP synthesis in which the polyoxoanion is linked covalently to the Au NPs via thiol group. A report by Keita et al. [46] highlights the results of a metal nanostructure synthesis strategy that used POMs as both reducing and capping agents where the POMs served those two purposes.

Hegde et al. [47] reported a facile synthesis of Au NPs using radiolytic method where Au NPs were coated by thiol-derivatized POMs $[POM(SH_2)]^{4-}$ in DMF/water solution (Fig. 1). This system controlled the stability and growth of the NPs. The organosilyl derivative $[\gamma\text{-}SiW_{10}O_{36}(RSi)_2O]^{4-}$ [R = $-C_3H_6SH$], called as $[POM(SH_2)]^{4-}$, was synthesized by adding (3-mercaptopropyl) trimethoxysilane (HSC_3H_6–$Si(Ome)_3$ and Bu_4NBr to a solution of Keggin ion $K_8(\gamma\text{-}SiW_{10}O_{36}).\ 12H_2O$, in acetonitrile and water. They inferred that the formation of numerous shapes of these $[POM(SH_2)]^{4-}$-capped Au NPs was dependent upon (1) the composition of DMF/water solution and (2) the reduction rate.

The parent compound for $[POM(SH)_2]^{4-}$ synthesis is the deca-tungstosilicate $[SiW_{10}O_{36}]^{8-}$ which has four nucleophilic surface oxygen atoms. These anions are isolated as tetraalkylammonium salts and are soluble in organic solvents and mixtures of DMF/water. After functionalization, the basic unit of the POM comprises a hydrophilic polyanion and a hydrophobic thiol-terminating organic chain to which the NPs are covalently bonded [47].

Keita et al. [48] reported a one-step synthesis and stabilization of Au NPs with the simple oxothiometalate $[Mo_3(\mu_3\text{-}S)\ (\mu\text{-}S)_3(Hnta)_3]^{2-}$ ($Hnta^{2-}$ is the nitrilotriacetate ligand) in water at room temperature without any catalyst by reducing $HAuCl_4$ with $Na_2[Mo_3(\mu_3\text{-}S)\ (\mu\text{-}S)_3(Hnta)_3]^{2-}$ (Fig. 2). The simultaneous presence of Mo^{IV}, sulfide, and $Hnta^{2-}$ in this anion is anticipated to offer both rich redox chemistry for reducing $HAuCl_4$ and strong stabilizing

Fig. 1 Schematic representation of thiol-functionalized polyoxometalate $[POM(SH)_2]^{4-}$ (Reproduced from Ref. [47] with permission from Elsevier)

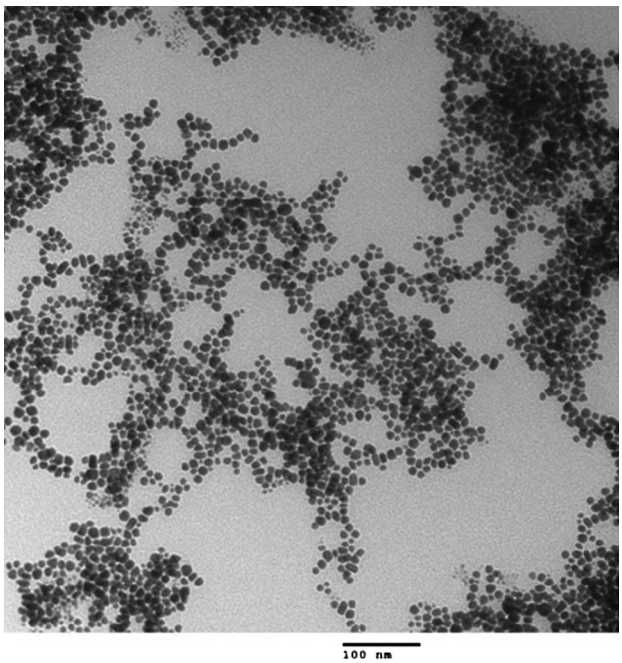

Fig. 2 TEM images of Au^0 nanoparticles synthesized by the reduction of $HAuCl_4$ with $Na_2[Mo_3(\mu_3\text{-}S)\ (\mu\text{-}S)_3(Hnta)_3]^{2-}$ (Reproduced from Ref. [48] with permission from Royal Society of Chemistry)

properties toward the resulting Au NPs, in environmentally benign conditions [49–51]. The pseudocuboidal $[Mo_3S_4]^{4+}$ core exhibited redox characteristics with the unique capability to incorporate various transition and post-transition metals (M′) to present a series of heterometallic complex derivatives containing the cuboidal $[Mo_3M'S_4]$ core [52]. Such a strategy might be a good route for the synthesis of mixed metal Au NP-based nanostructures.

Bao et al. [53] chose a wheel-shaped V^V–V^{IV} mixed-valence tungstovanadate $Na_{12}K_8H_4[K_8P_8W_{48}O_{184}\{V_4^V\ V_2{}^{IV}O_{12}(H_2O)_2\}_2]\cdot 80H_2O$ (V12) [54] to act as both the reducing agent and the stabilizer for the synthesis of Au NPs. The redox reaction of auric acid ($HAuCl_4$ (aq)) and V12 in water at room temperature without any catalyst provided Au NPs where the NP surface had absorbed a layer of V12 polyanions, rendering the Au NPs negatively charged with a relatively hydrophilic surface, confirmed by the zeta potential analysis. These materials were further fabricated into multilayer films based on the electrostatic attraction with the positively charged poly-ethyleneimine (PEI) via a layer-by-layer self-assembly.

Similarly, $[PMo_{12}O_{40}]^{4-}$ (HPMo) is able to transfer electrons efficiently to Au ions and reduce them to Au^0 (Eq. 1).

$$3[PMo_{12}O_{40}]^{3-} + Au^{3+} \rightarrow 3[PMo_{12}O_{40}]^{3-} + Au^0_{Colloid} \quad (1)$$

Ayati et al. [55] investigated the synthesis of Au nanostructures generated by a green chemistry process, using HPMo and $HPMo_{12-x}V_x$ as reductants in aqueous solution. The relative rates of reduction of Au^{3+} were in the order: $HPMo_9V_3 > HPMo_{10}V_2 > HPMo_{11}V >$ HPMo. The effect of Au ion concentration or molar ratio of HPMo to Au^{3+} on the size of Au NPs was studied. Addition of vanadium atoms to the POM used in this synthesis impacted the size and the shape of prepared NPs. From the TEM images, the NPs seem to be hexagonal and spherical in shape which shifts to anisotropic and irregularly shaped structures and to nanorods by an increase in the value of x in the $HPMo_{12-x}V_x$ formula.

Xu et al. [56] examined incorporation of metal NPs into dioctadecylamine (DOA)/12-molybdophosphoric acid (PMo_{12}) hybrid Langmuir–Blodgett (LB) film via in situ reduction of $HAuCl_4$ using PMo_{12} and observed that the gold ions are reduced to Au NPs in the hybrid film. Incomplete NPs' permeation into the film was explained as a result of larger volume of tetrachloroaurate ions and their negative charge, generating repulsion with the head groups of the surfactant. A regular structure of NPs incorporated on the hybrid LB film was obtained owing to good dispersion of Au ions over the LB film. The single monolayer generated from DOA–$HAuCl_4$/PMo_{12} shows a uniformly planar morphology even at high surface pressure. The establishment of Au NPs enhances the speed of photochromism, and PMo_{12} can cycle change to and from the mixed-valence heteropoly blue in the hybrid LB film after the formation of NPs [56].

Mixed-valence POMs also possess the potential to use them in the formation of NPs. In one study, one of mixed-valence POMs, β-$H_3[H_4P(Mo^V)_4(Mo^{VI})_8O_{40}]^{3-}$, was used in the one-pot synthesis as a reducing and capping agent in water at room temperature. They reported that this class of POMs can readily react with chloroauric acid at room temperature and the reaction can be monitored using its distinguishable color changes [57]. Figure 3 presents the morphological possibilities during the synthesis of Au^0 nanostructures by β-$H_3[H_4P(Mo^V)_4(Mo^{VI})_8O_{40}]^{3-}$ [57].

A significant number of studies have been performed regarding the preparation of POM-stabilized NPs, and the majority of strategies fall into the following categories: the reduction of noble-metal ions by reduced POMs where POMs play the role of the reducing and stabilizing agent [46, 58]; the reduction of noble-metal ion salts by a chemical reagent (H_2, $NaBH_4$, etc.) in the presence of POMs [59]; reduction of a metallic salt of the targeted metal by photo-reduced POMs, in the presence of an organic sacrificial donor; and the replacement of the stabilizing agents of preformed metallic NPs with POMs [60].

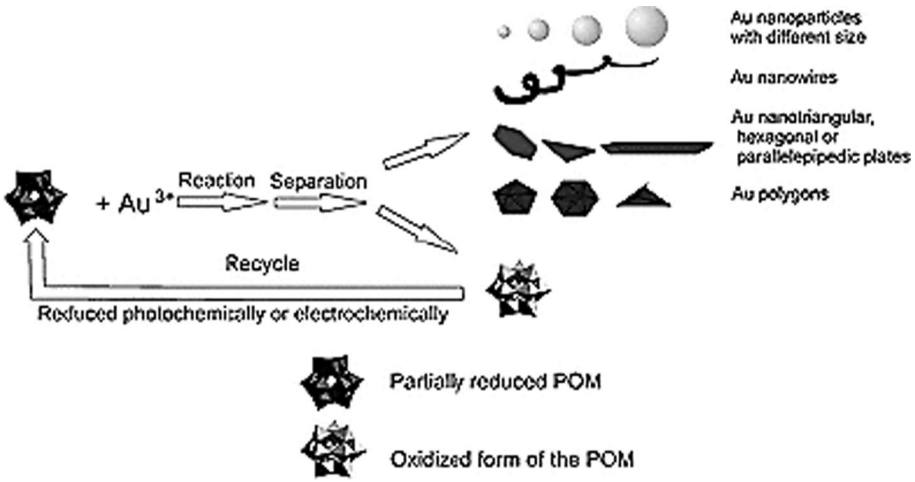

Fig. 3 Morphological possibilities during the synthesis of Au^0 nanostructures by β-$H_3[H_4P(Mo^V)_4(Mo^{VI})_8O_{40}]^{3-}$ and recyclability of the POM (Reproduced from Ref. [57] with permission from Royal Society of Chemistry)

Most of these studies were performed in aqueous solution and in the presence of other ligands or tetraalkylammonium counter ions, of which the latter are widely recognized as metallic NP stabilizers, thus the dual role of the POMs maybe slightly dubious [61]. In contrast, Au NPs are prepared under nonaqueous conditions and at relatively high temperature, not an environmentally sound approach. The route using POMs as sole reducing agents to synthesize Au NPs in water at room temperature is attractive from the perspective of sustainable practices. Numerous Au nanostructures, such as spherical [48] or quasi-spherical NPs [22], triangular and hexagonal nanoplates, twisted nanowires [57], and flower-like NPs [62], have been synthesized using appropriate POMs and modifying the concentrations or mole ratio of POMs without any additional reducing or stabilizing agents. Usually, the selected POMs are needed to be reduced by electrochemistry or photochemistry prior to synthesis process of Au NPs (vide infra).

Cryo-TEM imaging of POM–Au hybrid materials

The utility of cryo-electron microscopy (cryo-TEM) is because the technique image samples that have not been fixed or stained in any way, revealing them in their indigenous environment, e.g., for colloids such as POMs-NPs, a vitrified, frozen-hydrated state, very close to their native state [63]. Wang et al. [64] used POM anions, along with cryo-TEM imaging, spectroscopy, and other solution-state methods [65], to present the first detailed account of the thermodynamics, kinetics, growth, and surface organization of a structurally characterized protecting ligand shell on Au NPs. Their work addressed a number of POMs whose structures and charges were systematically altered. The POM anion shells were achieved by ligand exchange from citrate-encapsulated 13.8 nm Au NPs. The effects of anion charge on rates of initial association with the Au surface, relative importance of ligand structure versus charge on binding to Au atoms on the NP surface, monolayer growth and stability, and the part of counter cations and electrostatic interactions inside the inorganic polyelectrolyte ligand shell were studied. Cryo-TEM images (Fig. 4) indicate that monolayer growth happens through "islands," a mechanism that points to cation-mediated attraction between bound POMs. The electric potential barrier of the citrate-stabilized particles inhibits the rate of POM association with the Au surface. The linear increase of the binding affinities with the charges of structurally different POM anions suggested that no single orientation was needed for monolayer self-assembly.

Wang et al. [66], again in this context, addressed POM ligand lability by cryo-TEM imaging of monolayers of α-$AlW_{11}O_{39}^{9-}$ on 5.4-nm (smallest)-diameter Au-core NPs. In determining the selectivities and turnover rates of POM-protected metal NPs in catalysis, the function of ligand lability and reversible binding, along with the thermodynamics of monolayer formation, was examined. The binding affinities of α-$K_9AlW_{11}O_{39}$ and α-$Na_5AlW_{12}O_{40}$ were achieved by Langmuir isotherms, and the relative labilities of the two ligands were evaluated by UV–Vis analysis of alterations in surface plasmon resonance (SPR) upon adding citrate. The substitution of citrate by POM ligands at the Au surface leads to a significant increase in the extinction coefficient related to the maximum of the SPR at approximately 526 nm (Fig. 5), as a result of the large difference between the refractive indices of the organic (citrate) and inorganic (POM) ligands and their monolayers. Data provided revealed that the monolayers of α-$K_9AlW_{11}O_{39}$ (and its counter ions) [64, 67] possess substantial kinetic stability, whereas α-$Na_5AlW_{12}O_{40}$ is substantially more labile.

The same group used three representative POM anions and a series of alkali metal cations to determine that POM

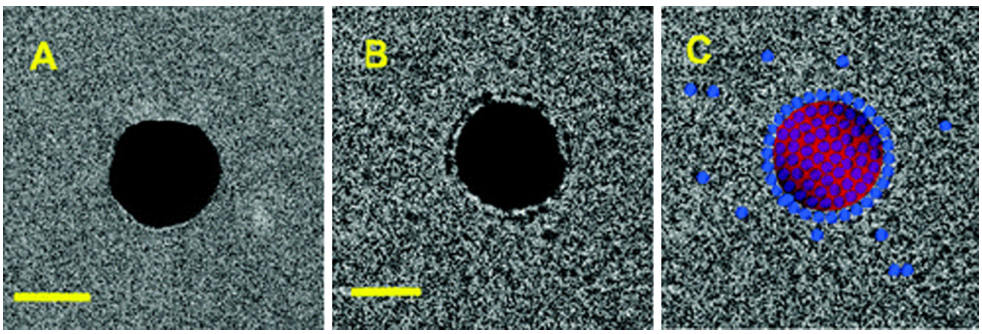

Fig. 4 Cryo-TEM images of (**a**) citrate-protected and (**b**) [α-$AlW_{11}O_{39}$]$^{9-}$-protected gold nanoparticles. **c** is a copy of the image in **b**, enhanced (*solid blue circles*) to highlight (1) the band of individual [α-$AlW_{11}O_{39}$]$^{9-}$ anions at the fringe of the gold particle, (2) coverage of the particle's surface indicated by the presence of this band, and (3) "freely solvated" molecules of [α-$AlW_{11}O_{39}$]$^{9-}$ held in the vicinity of the gold particle in the water–glass matrix. *Scale bar* 10 nm (Reproduced from Ref. [64] with permission from American Chemical Society) (Color figure online)

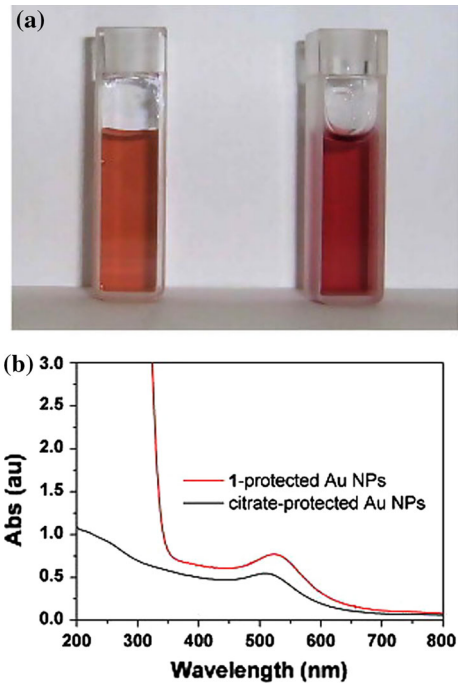

Fig. 5 **a** Photographs and **b** spectra of citrate-protected Au NPs and α-$K_9AlW_{11}O_{39}$-protected Au NPs. The cuvette at the left in **a** contains citrate-protected Au NPs. Addition of α-$K_9AlW_{11}O_{39}$ to a final concentration of 2.5 mM causes a visible color change (cuvette at *right*). Corresponding UV–Vis spectra are shown in **b** (Reproduced from Ref. [66] with permission from Elsevier) (Color figure online)

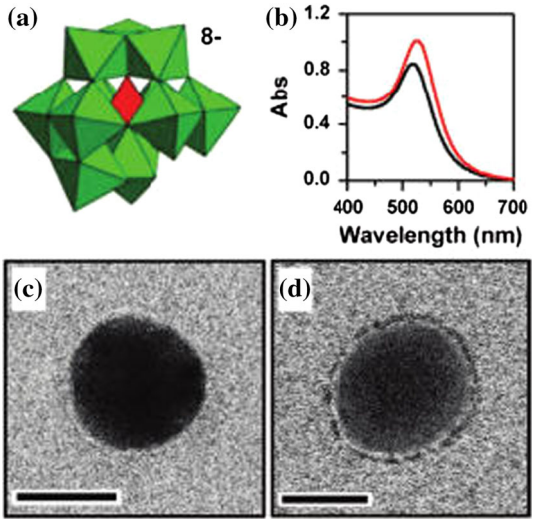

Fig. 6 Reaction of α-$SiW_{11}O_{39}^{8-}$ with a citrate-stabilized, 14-nm-diameter Au NP: **a** structure of α-$SiW_{11}O_{39}^{8-}$ (polyhedral notation); **b** UV–vis spectra of citrate-stabilized Au NPs before (*black*) and after (*red*) monolayer formation by α-$SiW_{11}O_{39}^{8-}$; **c** and **d** cryo-TEM images of citrate- and α-$SiW_{11}O_{39}^{8-}$-protected Au NPs, respectively. *Bar* 10 nm (Reproduced from Ref. [68] with permission from American Chemical Society) (Color figure online)

monolayer stability constant, K, varies with the size and properties of the cations in the same order as the one noticed for cation–anion association with α-$SiW_{11}O_{39}^{8-}$in solution: $Li^+ < Na^+ < K^+ < Cs^{+8}$ [68]. The Cryo-TEM images presented strong evidence that the POM monolayers are electrostatically stabilized (ionic) shells, suggestive of monolayer walls of "hollow" POM macroanion vesicles. These results can be extended and employed to predict self-assembly of metal oxide cluster anion-protecting ligand shells on Au NPs as confirmed by the cryo-TEM images (Fig. 6).

Cryo-TEM imaged well-formed POM monolayer shells on aqueous Au NPs in recent work [69]. Evidence for specific binding modes is found from data on stability criteria [70] and surface-enhanced Raman spectroscopy [71]. Sharet et al. [23] used cryo-TEM in order to determine the orientation of POMs on NP surface examining three different monolayer shells; each constituted of POMs with discrete sizes and shapes. The electron micrograph images revealed that the POM monolayer shells change with cluster anion size and shape. From examination of the images (Fig. 7) and statistical analysis of measurements

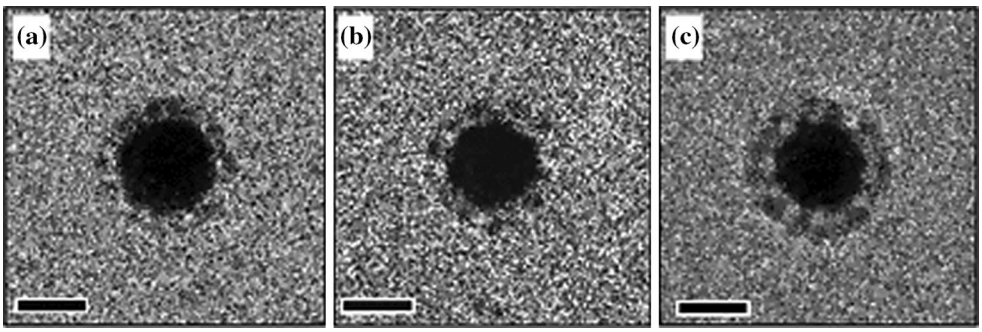

Fig. 7 Cryo-TEM images of the Au–POM core–shell structures. The 6.6-nm-diameter gold cores (*dark*) are surrounded by monolayer shells of **a** $[\alpha\text{-}AlW_{11}O_{39}]^{9-}$, **b** $[NaP_5W_{30}O_{110}]^{14-}$, and **c** $[P_4W_{30}Zn_4(H_2O)_2O_{112}]^{16-}$. *Scale bar* 5 nm (Reproduced from Ref. [23] with permission from Royal Society of Chemistry)

from many particles (Fig. 8), it was revealed that the $[NaP_5W_{30}O_{110}]^{14-}$ was bound "face down" with its C_5 axis perpendicular to the Au surface, while the long axis of the $[P_4W_{30}Zn_4(H_2O)_2O_{112}]^{16-}$ was tilted by ca. 60°.

These measurements contributed to the understanding of organization of structure and reactivity relationships for POM-protected metallic NPs [21, 22, 41, 70], a rising category of catalytically active nanostructures. Data acquired on 14-nm-diameter Au NPs provided a structural model involving the detailed internal incorporation of counter cations into the POM monolayer itself [64]. Consequently, POM-protected metal NPs may be regarded as crucial members in a domain [67] of electrostatically stabilized structures arraying from spherical single walls of hollow POM vesicles [72] to the two-dimensional arrangements of POMs on planar surfaces [73]. From such an electrostatic model, the stabilities of the POM monolayers on Au NPs are expected to change with the incorporated counter cation, in a similar fashion as lattice enthalpies of crystalline POM salts and energies of cation association change with POMs in solution [74].

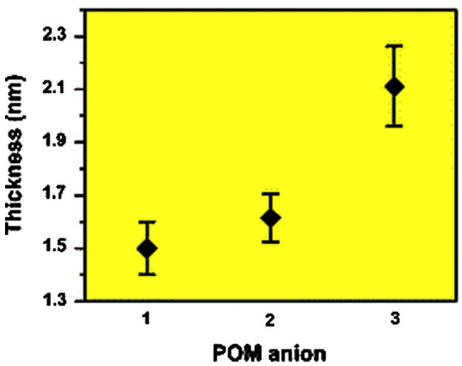

Fig. 8 Shell thicknesses for the monolayers of three POM ions, $[\alpha\text{-}AlW_{11}O_{39}]^{9-}$ (1), $[NaP_5W_{30}O_{110}]^{14-}$ (2), and $[P_4W_{30}Zn_4(H_2O)_2O_{112}]^{16-}$ (3) (Reproduced from Ref. [23] with permission from Royal Society of Chemistry)

Recent applications of POM–Au NPs hybrid materials

Photocatalysis

Troupis et al. [22] made substantial contributions to this area by synthesizing Au metal nanoclusters using the POM $[SiW_{12}O_{40}]^{4-}$as both stabilizer and photocatalyst. These studies presented a vital insight into the role of POMs as stabilizers for nanoclusters. In the case of Troupis et al. [22], the POMs are required to be photoactive but unfortunately not many POMs are photoactive. Also in the case of Mayer et al. [45], a suitable thiolate mediator group is required to pre-functionalize the POMs.

Niu et al. [75] prepared Au NPs by photoreduction in the presence of transition metal monosubstituted Keggin heteropolyanions ($PW_{11}M$) acting as photocatalyst, reducing agent, and stabilizer [75]. Their results revealed that the formation rate and morphology of the NPs strongly relied on preparation conditions, such as irradiation time, reductant (2-propanol) amount, and the type of transition metal substituted in the Keggin ion. Preparation conditions are critical in the synthesis of NPs, including the amount of reductant, irradiation time, stirring rate, reaction temperature, and counter ions [76]. An increase in the 2-propanol concentration and the irradiation time can shorten the formation time and make a more uniform morphology of the NPs. The authors proposed that extending the irradiation time encourages the generation of reduced $PW_{11}Fe$, leading to Au NP formation. When the irradiation time was prolonged, the Au NPs formed are too large to be stable, resulting in ready sintering and precipitation. Figure 9 indicates the differences in UV–Vis spectra of the Au NP solutions prepared in the presence of $PW_{11}M$ with two irradiation times [75].

Li et al. [77] developed a novel "green" catalytic system for the catalytic oxidation of organic pollutants. This system was made of three components; Au NPs were fixed on

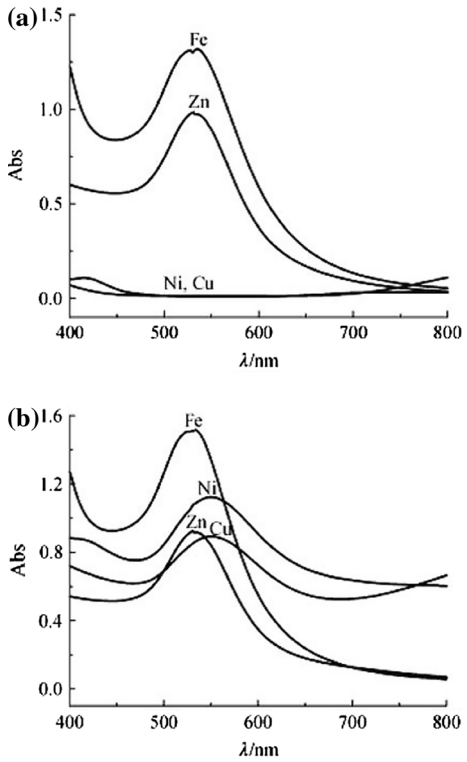

Fig. 9 UV–Vis spectra of the gold nanoparticle solutions synthesized in the presence of $PW_{11}M$ ($M = Zn^{2+}$, Fe^{3+}, Ni^{2+}, Cu^{2+}) with an irradiation time of 40 min (**a**) and an irradiation time of 90 min (**b**) (Reproduced from Ref. [75] with permission from Springer)

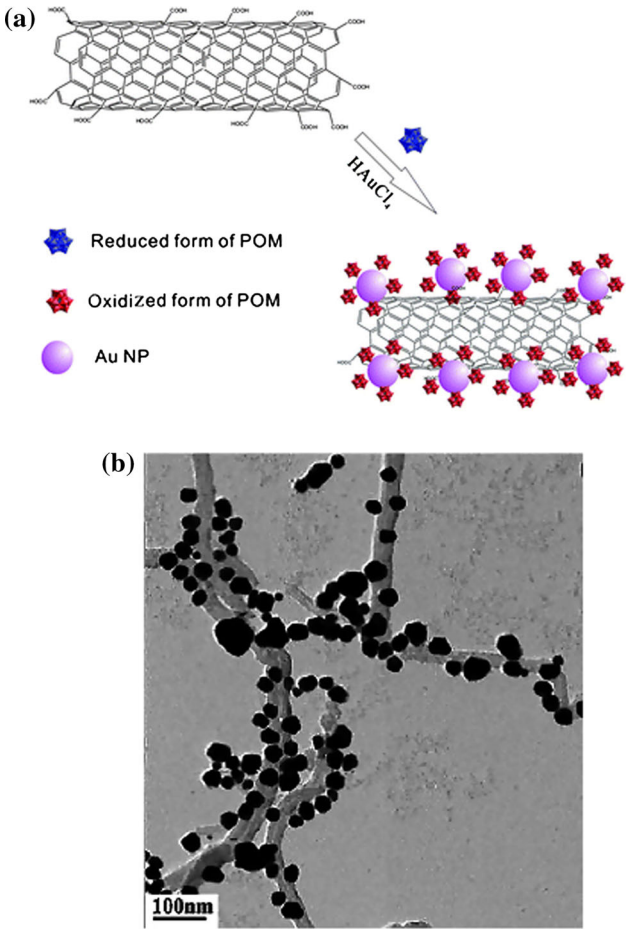

Fig. 10 **a** Schematic illustration of POMs serving as reducing, encapsulating, and bridging molecules. **b** Au NP@POM–CNT composites (Reproduced from Ref. [77] with permission from Royal Society of Chemistry)

carbon nanotubes (CNTs) using POMs as the binding agent to build metal NPs@POM–CNTs tricomponent nanohybrids. The pure Au NPs exhibited no photocatalytic activities, but the tricomponent CNTs/POM/Au NPs nanohybrids showed high photocatalytic activity under visible wavelengths, albeit with slow kinetics. A key step in the proposed mechanism is the excitation of the SPR of the Au NPs followed by charge transfer from the Au NPs to POMs. This visible light-induced electron transfer empowers the Au NPs to have significant oxidizing ability [77]. The Keggin-type $H_3PW_{12}O_{40}$ was employed to serve as a reducing, encapsulating, and bridging molecule (Fig. 10a, b).

This scheme has critical requirements, i.e., knowledge of the pH required for stability of the POM in its oxidized and reduced states and a reasonable match between the redox potentials, so that the electron transfer proceeds in the desired direction.

Reports of the use of other, more benign, and environment friendly POMs [22, 55, 78–83] have addressed the green synthesis/fabrication of Au NPs. Ayati and Bamoharrem have performed much work in this area [55, 79, 80]. Ayati et al. used Preyssler acid $H_{14}[NaP_5W_{30}O_{110}]$ as a single reagent to synthesize Au NPs (Fig. 11) [79] via a simple photoreduction technique. Preyssler acid is suited for this purpose owing to its properties including acidity, thermal and hydrolytic stability, reusability, high oxidation potential, and relatively benign environmental nature [81]. Synthesis of these Au NPs was accomplished by photolysis of a de-aerated solution of chloroauric acid, Preyssler acid, and 2-propanol. These NPs were tested for photodegradation of methyl orange for which they showed reasonable catalytic activity. The synthesized Au NPs were smaller and more uniform if Preyssler acid was used instead of other POMs.

In 2012, Ayati et al. [80] continued this work with another study where uniform and size-controlled Au NPs were prepared by the simple photolysis of aqueous Preyssler/Au^{3+}/2-propanol, but the size of NPs changed with variations in Au ion concentration and molar ratio of 2-propanol and Preyssler acid to Au concentration. A faster reduction resulted in smaller, more uniform, and hexagonal Au NPs and a critical ratio of Au(III) to Preyssler acid was

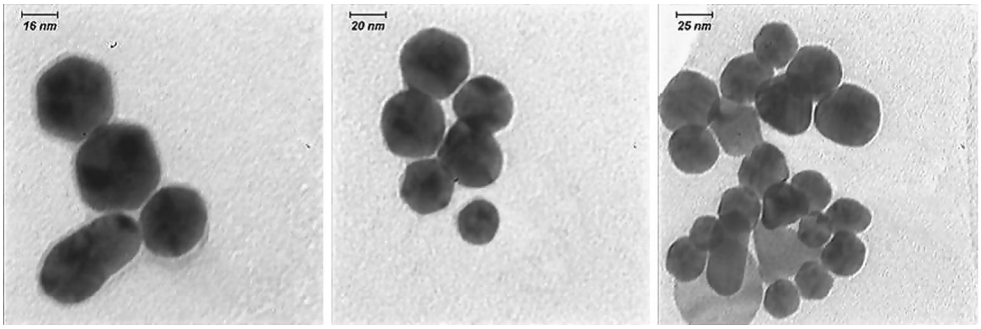

Fig. 11 TEM images of synthesized Au NPs after 45-min irradiation. Au NPs had a hexagonal morphology and 17 nm size (Reproduced from Ref. [79] with permission from Elsevier)

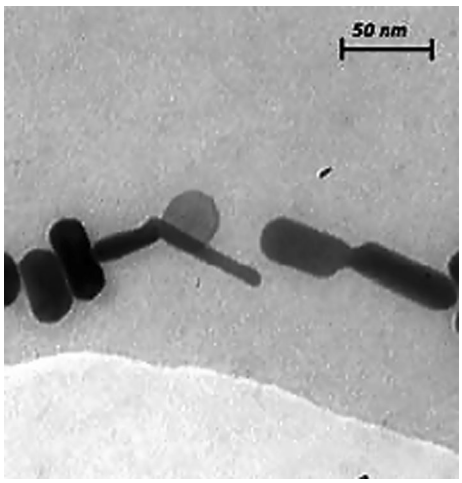

Fig. 12 TEM image of synthesized Au NPs (Reproduced from Ref. [84] with permission from author)

found. Below that ratio, smaller NPs formed and, above that ratio, larger particles were obtained. Among the three commonly employed POMs' structures Keggin ($H_3PW_{12}O_{40}$), Dawson ($H_6P_2W_{18}O_{62}$), and Preyssler ($H_{14}[NaP_5W_{30}O_{110}]$), the latter revealed highest activity, and the resulting particles were smaller and more uniform.

Ayati et al. [84] also used vanadium-substituted mixed addenda POMs ($H_6[PMo_9V_3O_{40}]$, $HPMoV_3$) to synthesize Au nanorods via simple photoreduction, the photolysis of a de-aerated solution of Au(III)/$HPMoV_3$/2-propanol. In the TEM image (Fig. 12), the shapes of the Au nanorods obtained appear almost uniform. The photoactive properties and robustness of these hybrid materials make them attractive as reagents to mediate redox or electron transfer reactions for many applications.

Olefin oxidation and hydrogenation

The Au–O bond is relatively unstable, as observed in the ready decomposition of Au_2O_3 at about 160 °C [85]. Chelating organic nitrogen donor ligands have been used for stabilization in the synthesis of most Au(III) oxo complexes [86]. Cao et al. presented two Au^{III}-containing heteropolytungstates, where the gold ion is octahedrally coordinated and possesses a terminal Au^{III} oxo bond [87]. Bagno and Bini pointed out that such a species is anticipated to be highly unstable and should exhibit extremely uncommon ^{183}W and ^{17}O NMR characteristics [88] based on a relativistic DFT computational study carried out by them. The weak Au^{III}–O bond should be highly reactive perhaps acting as oxygen donors in oxidation reactions such as the epoxidation of olefins [89].

Izarova et al. [90] reported a totally inorganic distinct heteropolyaurate $\left[Au_4^{III}As_4^{V}O_{20}\right]^{8-}$ (Fig. 13), prepared in aqueous medium at room temperature and isolated as a hydrated sodium salt $Na_{13}\left[(H_2O)_4(NO_3)_2Na_5\left\{Au_4^{III}As_4^{V}O_{20}\right\}_2\right]\cdot 39H_2O$. They suggested that $\left[Au_4^{III}As_4^{V}O_{20}\right]^{8-}$ could be used as an effective catalyst (or model for one) in heterogeneous Au-based oxidations using molecular oxygen, but they reported no experiment on any catalytic ability.

D'Souza et al. [34] reported the chemical synthesis of Au metal nanoclusters using either tetraalkylammonium salts of the heteropolyoxotungstates $[\alpha\text{-}PW_{12}O_{40}]^{3-}$ (PW_{12}), $[P_2W_{18}O_{62}]^{6-}$ (P_2W_{18}), or their lacunary derivatives $[\alpha\text{-}PW_{11}O_{39}]^{7-}$ (PW_{11}) and $[P_2W_{15}O_{56}]^{12-}$ (P_2W_{15}) as stabilizers, through chemical reduction in acetonitrile solvent (Fig. 14). They observed that the rate of reaction depended on the polyoxotungstate used in the order $P_2W_{18} > P_2W_{15} > PW_{12} > PW_{11}$. Catalytic activity of stabilized Au nanoclusters has not been studied for these POMs although similarly structured Pd nanoclusters exhibited activity in hydrogenation of alkenes. Figure 14 shows a proposed electrostatic stabilization model for these colloids, with the negatively charged POM and a layer of positively charged tetrabutylammonium ions able to stabilize the NPs [43]. These cations are also responsible for the solubility of the nanocluster system in acetone or acetonitrile [45].

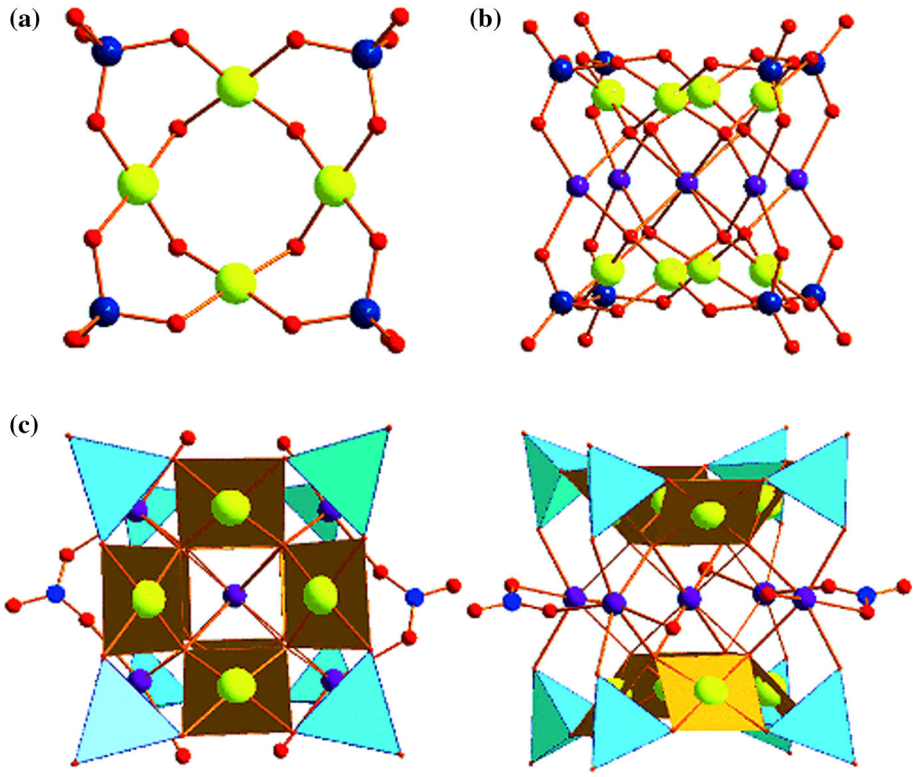

Fig. 13 Ball-and-stick representation of **a** $\left[Au_4^{III}As_4^{V}O_{20}\right]^{8-}$ and **b** the $Na_5Au_8As_8$ fragment. **c** Combined ball-and-stick or polyhedral representation of the $[(H_2O)_4(NO_3)_2Na_5Au_8As_8O_{40}]^{13-}$ dimeric assembly: top (*left*) and side (*right*) views. Au *yellow*, As *dark blue*, O *red*, Na *purple*, N *blue*; $\{AuO_4\}$ *dark yellow squares*, $\{AsO_4\}$ turquoise tetrahedral (Reproduced from Ref. [90] with permission from John Wiley and Sons) (Color figure online)

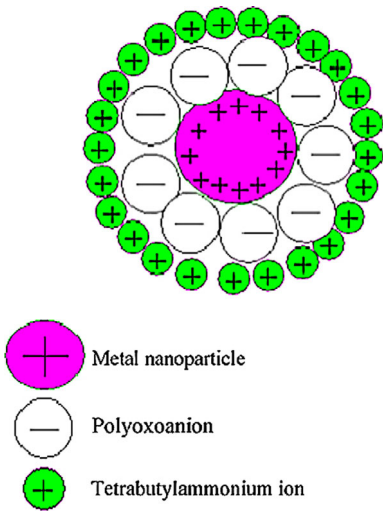

Fig. 14 Schematic of polyoxoanion-stabilized colloid (Reproduced from Ref. [34] with permission from Elsevier)

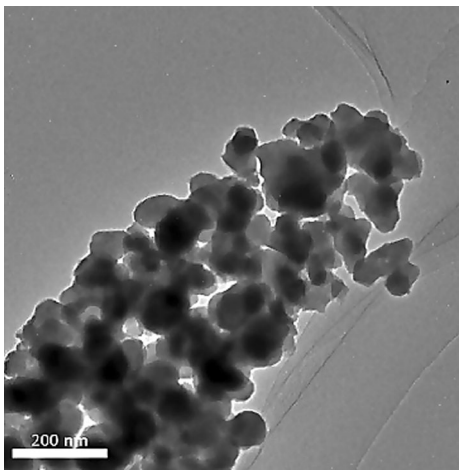

Fig. 15 Bright-field TEM image of the Au/BaPOM catalyst dried at 140 °C (Reproduced from Ref. [91] with permission from Royal Society of Chemistry)

Tebandeke et al. [91] reported Au NPs supported on salts of POMs (Fig. 15) for the epoxidation of olefins using molecular oxygen as an oxidant and *t*-butyl hydroperoxide as an initiator under solvent-free conditions. The catalysts gave high selectivity (>90 %) to epoxide formation for norbornene and cyclooctene but with rather low conversion. The catalyst was recyclable with no loss of activity affirming the stabilizing effect of the anionic POM support.

However, the insight into details of adsorption/activation of oxygen and/or organics on the Au NP surface was not reported. Further details are needed regarding the interaction of support and Au NPs and the redox behavior of the POMs to better understand the mechanism of oxidation and refine the catalyst. In general, these hybrid materials have shown much promise as catalysts because of the ability to tune the nature of the POMs and Au NPs and the relative robustness of the resulting hybrid material. Using these hybrids may promote reactions at mild conditions, without solvent, with less waste resulting in more environmentally sound manufacturing processes.

Biomass catalysis

Gold–polyoxometalate hybrid materials have been successfully employed for biomass catalysis. An et al. [92] reported the catalytic behavior of nanocomposites of Au NPs and Keggin-type POMs Au/$Cs_xH_{3-x}PW_{12}O_{40}$ for the conversion of cellobiose into gluconic acid (Fig. 16). These catalysts demonstrated higher selectivity for gluconic acid than Au catalysts supported on typical metal oxides but with slower conversion. They suggested that the acidity associated with the catalyst and mean particle size of the Au NPs played crucial roles in the conversion of cellobiose into gluconic acid. The acidic sites were expected to catalyze the hydrolysis of cellobiose, forming glucose as an intermediate, and the Au NPs were responsible for the oxidation of glucose into gluconic acid. Catalysts with smaller Au NPs showed higher conversions, and a gluconic acid yield of 97 % was obtained with Au NPs' size of 2.7 nm. Limitations associated with the instability of the system over long-term hydrothermal conditions led to catalyst deactivation upon repeated use. One explanation might be the loss and sintering of Au NPs or the detachment from POMs with repeated use.

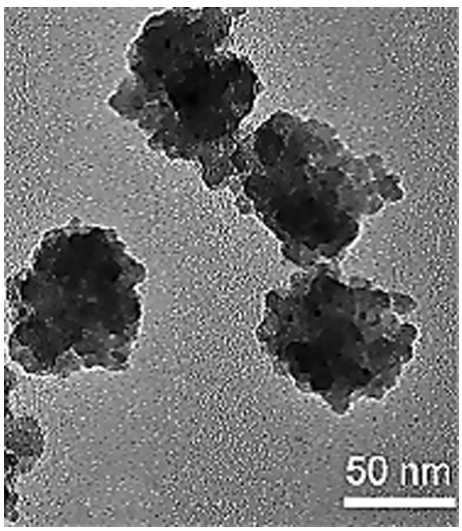

Fig. 16 A typical TEM micrograph for Au/$Cs_xH_{3-x}PW_{12}O_{40}$ (Reproduced from Ref. [92] with permission from John Wiley and Sons)

Electrode materials

The assembly of POMs and Au NPs onto electrode surfaces and the use of these electrodes in electrocatalysis is another, quite interesting, application of this class of hybrid material. Nadjo and coworkers' team [46, 49, 93] deposited solutions of POM-protected metal NPs onto electrode surfaces, allowed them to dry, coated the obtained films with nafion, and then employed these nano-engineered films as electrocatalysts for numerous reductive processes. Reports regarding the formation and structures of electrostatically stabilized POM monolayer protecting shells on Au NPs [64, 66, 75, 94] provide inspiration for the design of functionalized electrodes for both analytical and synthetic purposes (Fig. 17).

Babakhanian et al. [95] constructed a polypyrrole-modified electrode based on α-POM ($K_7PMO_2W_9O_{39}\cdot H_2O$) incorporating Au NPs (Fig. 18). This design exploits the electron pathway effect of α-POM and known properties of Au NPs in electrochemical sensing coupled with the conductive properties of polypyrrole film. The PPy–α-POM–AuNP-modified Au electrode proved to be very successful for sensitive monitoring and quantification of folic acid in

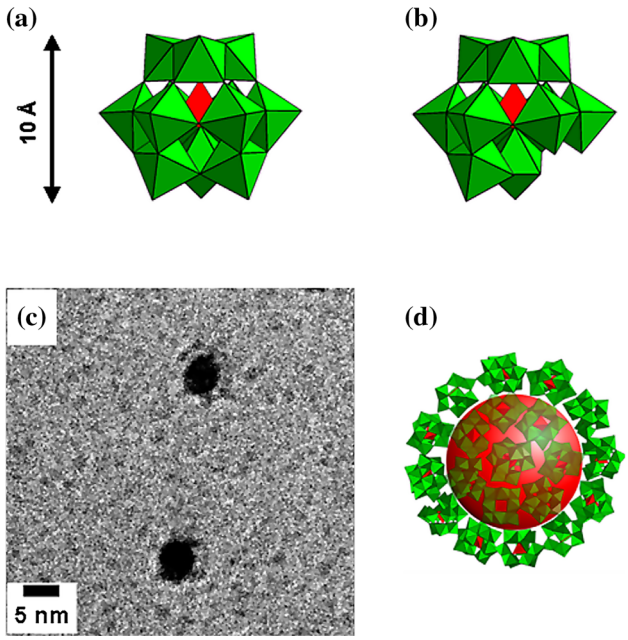

Fig. 17 **a** Polyhedron representations of α-$AlW_{12}O_{40}^{5-}$, a plenary Keggin anion. **b** α-$AlW_{11}O_{39}^{9-}$, its monolacunary derivative. **c** Cryo-TEM image of α-$AlW_{12}O_{40}^{5-}$-protected Au NPs. **d** Cartoon illustration of the monolayer shell of α-$AlW_{12}O_{40}^{5-}$ in the periphery of the gold core (Reproduced from Ref. [66] with permission from Elsevier)

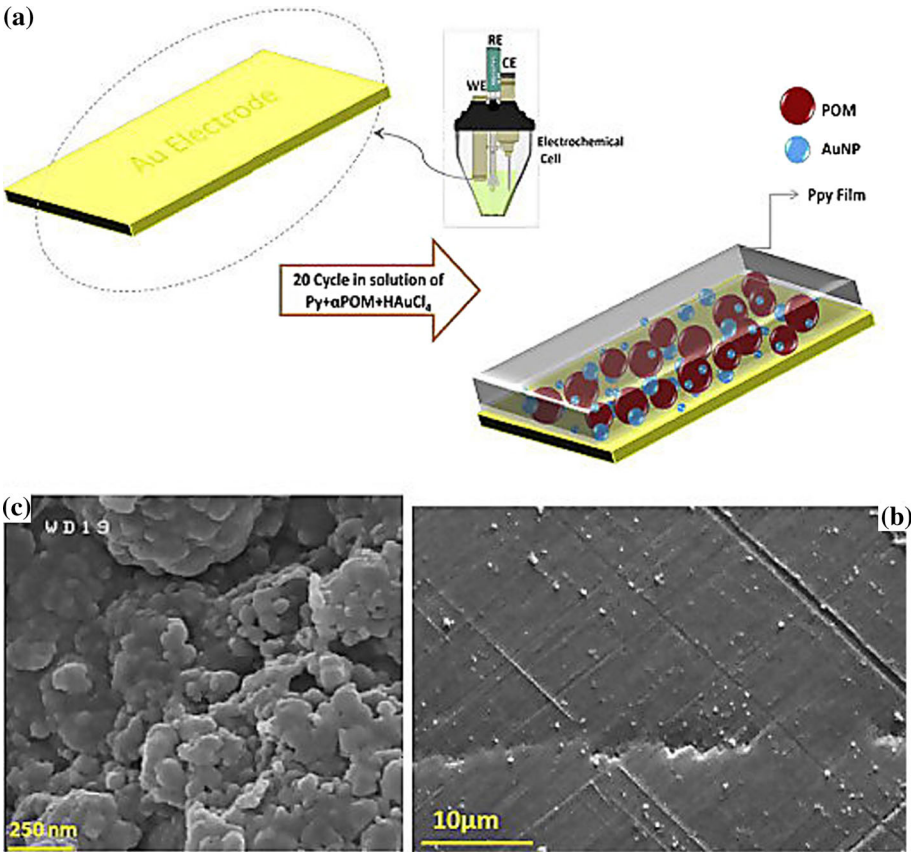

Fig. 18 Overall scheme for the preparation of the PPy–α-POM–AuNP film-modified Au electrode (**a**), SEM image for bare Au(C), and Au/PPy–α-POM–AuNPs (**b**)-modified electrodes (Reproduced from Ref. [95] with permission from Elsevier)

the supplements and human blood serum samples with side interferences at more positive reduction potentials not obtained by other sensors. This result supports this general design for functionalized electrodes in biological and non-biological applications at physiological pH. The composite films are readily prepared on the surface of the electrode with NPs through electropolymerization of pyrrole. The Au NPs' synthesis is accomplished with α-POM which serves as an electron and proton source [96].

Photoelectrochemical water splitting mediated by POMs–NPs has been observed [97]. Solarska et al. [98] studied Keggin-type phosphododecamolybdate ($PMo_{12}O_{40}^{3-}$) anion-capped Au NPs of uniform sizes ranging from 30 to 40 nm (Fig. 19) for improving sunlight-induced water splitting in thin-film tungsten trioxide (WO_3) photoanodes. The combined plasmonic and catalytic property of Au NPs attached to the WO_3 surface led to an increase in water photooxidation currents. Keggin-type POMs, such as $PMo_{12}O_{40}^{3-}$, display good proton conductivity and have the ability to undergo stepwise, reversible multi-electron transfer reactions [99]. The negatively charged $PMo_{12}O_{40}^{3-}$ anions organized as a ca. 1–2-nm-thick film on the Au NPs prevented the sintering of Au NPs to some extent due to their bulk and electrostatic repulsion. These anions are believed to occupy a limited count of active catalytic sites on the NP surfaces and interact with the Au via corner oxygen atoms as observed in TEM images (Fig. 20b) where the capped Au NPs are organized around the large size WO_3. The polyoxomolybdate anions form a covering self-assembled monolayer on the Au NP surface.

Zhang et al. [100] found that POM-monolayer-protected Au NPs could bind to electrode surfaces in a reversible manner, leading to a spectacular current amplification and well-behaved, quasi-reversible cyclic voltammetric behavior at extremely small electrolyte concentrations. This result provides incentive for research in electrocatalysis by dilute aqueous solutions of POM-protected Au NPs. However, additional research is required to better understand the mechanism(s) in electron transfer chemistry responsible for this phenomenon.

Zoladek et al. [32] studied the electro-oxidation of ethanol by impregnating titanium dioxide matrix with phosphododecamolybdate-modified (stabilized) Au NPs and combined them with catalytic nanostructured platinum. These POM-stabilized Au NPs were free of organic impurities [101] in comparison to the Au NPs prepared with stabilizing organic ligands. The negatively charged phosphomolybdate-modified Au NPs are electrostatically attracted to oxocationic species on titanium dioxide in acid media. The POM capping layers can also undergo multi-

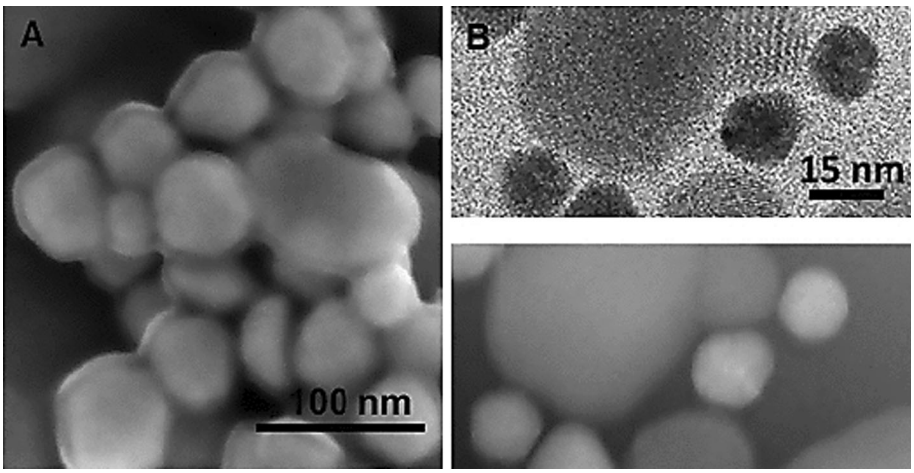

Fig. 19 **a** SEM and **b** TEM images of colloidal gold nanoparticles capped with phosphododecamolybdate adsorbates spread onto a conductive glass substrate (**a**) and onto a WO_3 film surface (**b**), and posttreated at 70 °C (Reproduced from Ref. [98] with permission from John Wiley and Sons)

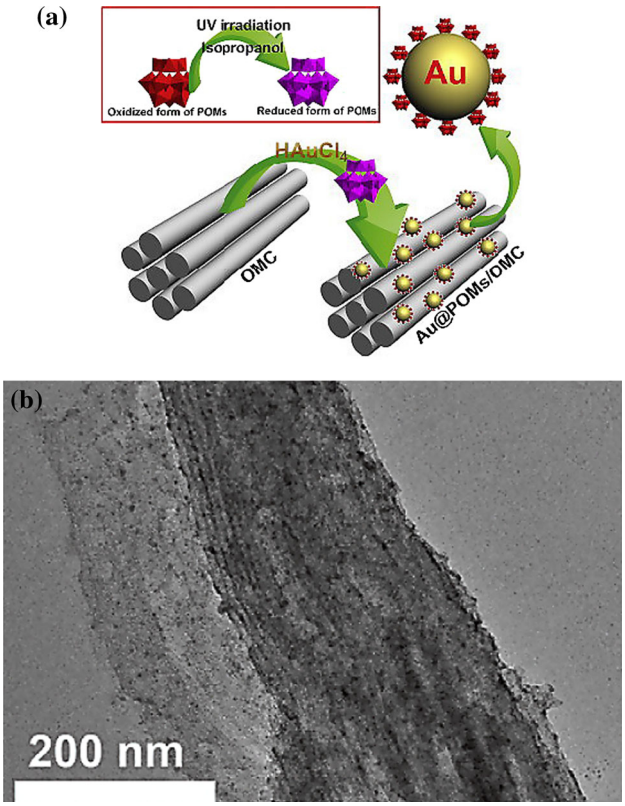

Fig. 20 **a** Illustration of the preparation of Au@POMs/OMC tricomponent nanohybrids. **b** A typical large-scale TEM image of Au@POMs/OMC (Reproduced from Ref. [117] with permission from Elsevier)

electron redox processes and perhaps activate the Pt-based electrocatalyst for the oxidation of ethanol in that fashion [102].

Zoladek et al. [103] prepared Au–PMo_{12} colloids by treating a partially reduced solution of heteropoly blue molybdate with an aqueous solution of $HAuCl_4$ as catalysts for the electro-oxidation of ethanol. The polymolybdate anions prevented Au NPs' agglomeration, and highly colored stable colloidal Au–PMo_{12} solutions were prepared. The Au–PMo_{12} NPs were employed as supports/carriers for dispersed platinum NPs, and an efficient electrocatalytic system was yielded. The factor which most affected the size and morphology of the NPs was the synthesis temperature.

Bromate, a human carcinogen, can be present in drinking water as a disinfection side product of chlorination and ozonation [104]. Ernst et al. [105] used PMo_{12}-protected Au NPs as a catalyst for bromate reduction. Au NPs protected initially by alkane thiols in nonaqueous solvent were exchanged by ligand exchange and liquid–liquid extraction into aqueous solution to yield Au NPs protected by PMo_{12}, with no change in the size of NPs. Glassy carbon electrodes modified with these PMo_{12}–Au NPs effected the ready reduction of bromate.

This group [101] extended the system to address reduction of hydrogen peroxide. The NPs were linked into hybrid organic–inorganic 3-dimensional networks on glassy carbon electrode by the use of positively charged conducting polymer bridges. The underlying idea was based on multiple formations of two-dimensional groups made up alternately of polypyrrole layers or ultra-thin PANI [106, 107] and AuNP–PMo_{12}. The polymer bridges [108, 109] are expected to increase the stability and dispersion of metal particles. This PMo_{12}–Au NPs–PPy composite film demonstrated electrocatalytic activity for H_2O_2 reduction higher than that observed for bare Au electrode.

Wiaderek et al. [110] also worked to develop an electrocatalytic system for the reduction of bromate by synthesis of Au NPs stabilized with an adsorbed layer of Rh_2PMo_{11} in order to determine if Au NPs enhanced the electrocatalytic activity of Rh_2PMo_{11}. They also developed modified electrodes which are stabilized in hydrodynamic situations, such as a flowing electrolyte. The Au NPs–

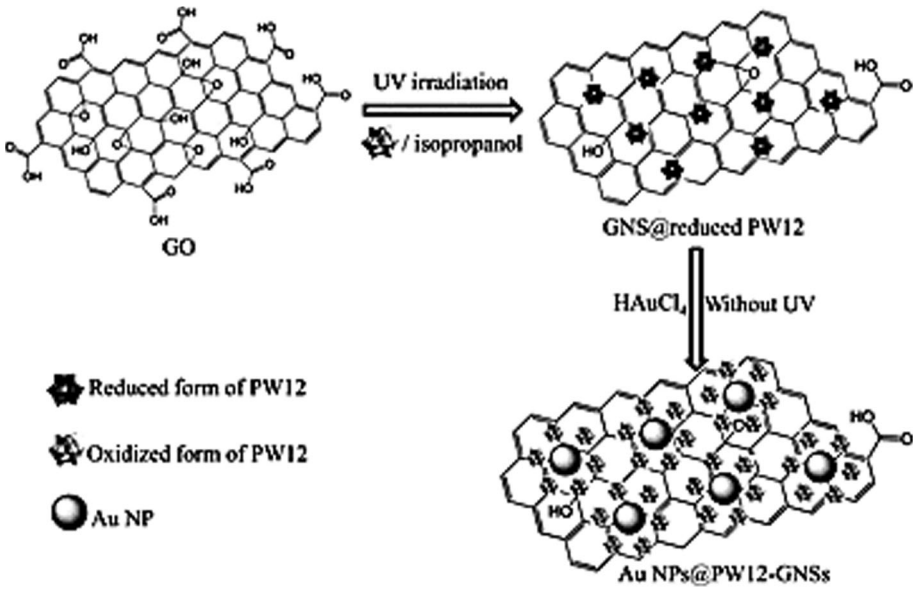

Fig. 21 Preparation procedure of representative tricomponent Au NPs@POM–GNSs nanohybrids (Reproduced from Ref. [54] with permission from John Wiley and Sons)

Rh_2PMo_{11} mediated oxidations, but the NPs were adsorbed very weakly to permit direct modification of electrode materials. To address this problem, the glassy carbon electrode was modified with 3-aminopropyltriethoxysilane (APTES) followed by electrostatic assembling with Au NPs–Rh_2PMo_{11}. The addition of Au NPs increased the current for bromate reduction by a factor of 2.5 relative to that at glassy carbon electrode/Rh_2PMo_{11}.

Bio-sensing

Hydrogen peroxide (H_2O_2) is a reactive oxygen species as an essential mediator [111] and by-product of many oxidative biological processes. Nicotinamide adenine dinucleotide (NADH) is a vital coenzyme in metabolic processes, widely present in every cell of organisms, and acts as a hydrogen and electron carrier in photosynthesis and cellular respiration. The investigation of the redox reactivity of NADH is crucial as many dehydrogenase enzymes use these compounds as cofactors [112, 113]. Thus, the accurate and quick detection of H_2O_2 and NADH is of great importance.

Most electrochemical biosensors are based on enzymes [114]; however, enzyme-based biosensors have downsides, for instance a complex structure that increases price, and low stability due to the inherent nature of enzymes [115] and the use of enzyme-free biosensors would be an attractive option. Au NPs are good contenders for enzyme-free electrochemical biosensors as they possess good electrical conductivity, which makes fast electron transfer possible, good electrocatalytic properties, and a high surface area, all factors imperative for realizing high sensitivity [116].

Zhang et al. [117] also presented a facile one-pot synthesis of Au NPs with POM $H_3PW_{12}O_{40}$ (PW_{12}) and ordered mesoporous carbon (OMC) to give Au@POMs/OMC. This material is a tricomponent nanocomposite (Fig. 20a, b), where the POMs served as reducing agents for Au(III) and bridging molecules for Au NPs and OMC [77, 118]. They believed that Au@POMs/OMC can exhibit enhanced electrocatalytic activities, because of the collaborative effects of Au NPs and OMC materials. The amperometric measurements indicated that these materials possess a reasonable catalytic activity with sensitivity, stability, range, low detection limit, and good response to acetaminophenol, H_2O_2, and NADH detection suggesting that these show promise as enzyme-free biosensors. These materials and more of their kind could be used as an electrochemical sensing platform for biomolecules and suggest new approaches to the development of novel electrode materials.

Much interest has been paid to the development of both enzymatic [119] and enzyme-free [120] hybrid Au–GNS (graphene tricomponent nanohybrids)-based biosensors. Liu et al. [54] presented a facile approach (Fig. 21) to prepare nanohybrid Au NPs@POM–GNSs materials with a Keggin-type ($H_3PW_{12}O_{40}$) POM as the sole component to bind Au NPs on graphene tricomponent nanohybrids (GNSs). The electrostatic repulsion between negatively charged POMs prevents Au NPs from aggregating [121]. As a preliminary test of their electrocatalytic behavior, these novel nanohybrids were employed as enzyme-free biosensors for H_2O_2 detection and showed satisfactory results. Another application of POM–Au hybrid materials, i.e., a polypyrrole-modified electrode, based on α-POM ($K_7PMO_2W_9O_{39}{\cdot}H_2O$) and its incorporation with Au NPs for sensitive monitoring and quantification of folic acid in the supplements and human blood serum samples [95] is discussed. This type of hybrid materials may provide a new

class of applicable biosensors, e.g., glucose monitoring, food analysis, DNA bio-sensing, microbial bio-sensing, and ozone bio-sensing to name a few.

Antibacterial drugs

POMs are known in the field of medicine because of their antibacterial, antiviral, and anticancer behavior [122–124]. Daima et al. [125] prepared tyrosine-reduced Au NPs^{Tyr} by employing a "green" approach. The preparation required the aqueous reaction of tyrosine and surface functionalization of the Au NPs by the use of one of two different POMs (12-phosphotungstic acid (PTA) or 12-phosphomolybdic acid (PMA)), followed by further modification of the nanomaterials using lysine to provide appropriate activity. Important aspects of this system are as follows: Au NPs^{Tyr} is the carrier and stabilizer for the antimicrobial component (POMs); the presence of the cationic amino acid lysine in the outermost shell aids in binding these nanomaterials to the negatively charged bacterial cells. A sequential surface functionalization approach using POMs and lysine onto biocompatible Au NPs was used (Fig. 22). *E. coli* was used as a model bacterium to evaluate the effective antibacterial activities of these functionalized nanomaterials. This work productively showed that even highly biocompatible substances such as gold can be made highly antimicrobial and cytotoxic by employing simple ligands such as POMs and lysine to their surface by a sequential functionalization. The sequential nature of the functionalization suggests that such a route is a versatile path to many different agents.

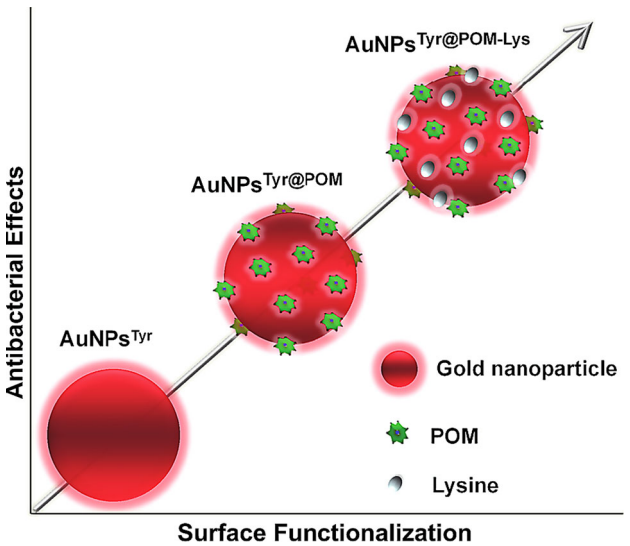

Fig. 22 Schematic representation of the summary outcome of this work showing increase in antimicrobial activity of Au NPs after their sequential functionalization with POMs and lysine (Reproduced from Ref. [125] with permission from Plos One)

Conclusions

POMs have a significant importance in the preparation and stabilization of NPs, attributed to their dual nature as both reducing and capping agents. The unique structure and properties of POMs are responsible for their current and future applications over diverse fields. POM–Au NPs hybrid materials have successfully been employed for biocatalysis, electrocatalysis, photocatalysis, oxidation of alkenes, bio-sensing, and medicinal chemistry. Despite all of the applications of POMs to this point, their surface chemistry is still not well understood. The possible permutations of POM-stabilized Au NPs and the dynamic and complex surface chemistry they possess make them attractive targets for future study.

Acknowledgements This work was financially supported by the Zhejiang Province Natural Science Foundation (Y4080247), Natural Science Foundation of China (21376213), and Opening Project of Guangxi Key Laboratory of Petrochemical Resource Processing and Process Intensification Technology (K002). We thank Professor Wayne Tikkanen from California State University and Professor Zhan Lin from Zhejiang University to make great contributions to the manuscript.

Compliance with ethical standards

Conflict of interest The authors declared that they have no conflict of interest.

References

1. Cozzoli PD, Pellegrino T, Manna L (2006) Synthesis, properties and perspectives of hybrid nanocrystal structures. Chem Soc Rev 35:1195–1208
2. Kolb U, Quaiser SA, Winter M, Reetz MT (1996) Investigation of tetraalkylammonium bromide stabilized palladium/platinum bimetallic clusters using extended X-ray absorption fine structure spectroscopy. Chem Mater 8:1889–1894
3. Bönnemann H, Richards RM (2001) Nanoscopic metal particles—synthetic methods and potential applications. Eur J Inorg Chem 10:2455–2480
4. Klabunde KJ (2001) Nanostructured materials in chemistry. Wiley, New York
5. Schmid G (2004) Nanoparticles: from theory to application. Wiley, New York
6. Daniel MC, Astruc D (2004) Gold Nanoparticles: assembly, supramolecular chemistry, quantum-size-related properties, and applications toward biology, catalysis, and nanotechnology. Chem Rev 104:293–346
7. Correa-Duarte MA, Liz-Marzán LM (2006) Carbon nanotubes as templates for one-dimensional nanoparticle assemblies. J Mater Chem 16:22–25
8. Huang J, Tao AR, Connor S, He R, Yang P (2006) A general method for assembling single colloidal particle lines. Nano Lett 6:524–529
9. Pastoriza-Santos I, Liz-Marzán LM (2009) N, N-Dimethylformamide as a reaction medium for metal nanoparticle synthesis. Adv Funct Mater 19:679–688

10. Kamat PV (2002) Photophysical, photochemical and photocatalytic aspects of metal nanoparticles. J Phys Chem B 106:7729–7744
11. El-Sayed MA (2001) Some interesting properties of metals confined in time and nanometer space of different shapes. Acc Chem Res 34:257–264
12. Hughes MD, Xu YJ, Jenkins P, McMom P, Landon P, Enache DI, Carley AF, Attard GA, Hutchings GJ, King F, Stitt EH, Johnston P, Griffin K, Kiely CJ (2005) Tunable gold catalysts for selective hydrocarbon oxidation under mild conditions. Nature 437:1132–1134
13. Cano I, Chapman AM, Urakawa A, van Leeuwen PVNM (2014) Air-stable gold nanoparticles ligated by secondary phosphine oxides for the chemoselective hydrogenation of aldehydes: crucial role of the ligand. J Am Chem Soc 136:2520–2528
14. Johnston JH, Nilsson T (2012) Nanogold and nanosilver composites with lignin-containing cellulose fibres. J Mater Sci 47:1103–1112. doi:10.1007/s10853-011-5882-0
15. Boronat M, Corma A (2010) Oxygen activation on gold nanoparticles: separating the influence of particle size, particle shape and support interaction. Dalton Trans 39:8538–8546
16. Deng YH, Cai Y, Sun ZK, Liu J, Liu C, Wei J, Li W, Wang Y, Zhao DY (2010) Multifunctional mesoporous composite microspheres with well-designed nanostructure: a highly integrated catalyst system. J Am Chem Soc 132:8466–8473
17. Deng X, Friend CM (2005) Selective oxidation of styrene on an oxygen-covered Au(111). J Am Chem Soc 127:17178–17179
18. Turner M, Golovko VB, Vaughan OPH, Abdulkin P, Berenguer-Murcia A, Tikhov MS, Johnson BFG, Lambert RM (2008) Selective oxidation with dioxygen by gold nanoparticle catalysts derived from 55-atom clusters. Nature 454:981–983
19. Gajan D, Guillois K, Delichere P, Basset JM, Candy JP, Caps V, Coperet C, Lesage A, Emsley L (2009) Gold nanoparticles supported on passivated silica: access to an efficient aerobic epoxidation catalyst and the intrinsic oxidation activity of gold. J Am Chem Soc 131:14667–14669
20. Alves L, Ballesteros B, Boronat M, Ramon Cabrero-Antonino J, Concepcion P, Corma A, Angel Correa-Duarte M, Mendoza E (2011) Synthesis and stabilization of subnanometric gold oxide nanoparticles on multiwalled carbon nanotubes and their catalytic activity. J Am Chem Soc 133:10251–10261
21. Maayan G, Neumann R (2005) Direct aerobic epoxidation of alkenes catalyzed by metal nanoparticles stabilized by the $H_5PV_2Mo_{10}O_{40}$ polyoxometalate. Chem Commun 36:4595–4597
22. Troupis A, Hiskia A, Papaconstantinou E (2002) Synthesis of metal nanoparticles by using polyoxometalates as photocatalysts and stabilizers. Angew Chem Int Ed 41:1911–1914
23. Sharet S, Sandars E, Wang Y, Zeiri O, Neyman A, Meshi L, Weinstock IA (2012) Orientations of polyoxometalate anions on gold nanoparticles. Dalton Trans 41:9849–9851
24. Pope MT (1983) Heteropoly and isopoly oxometalates. Springer, Berlin
25. Romero PG, Gallegos KC, Cantu ML, Pastor NC (2005) Hybrid nanocomposite materials for energy storage and conversion applications. J Mater Sci 40:1423–1428. doi:10.1007/s10853-005-0578-y
26. Hill CL, Prosser-McCartha CM (1995) Homogeneous catalysis by transition metal oxygen anion clusters. Coord Chem Rev 143:407–455
27. Pope MT, Muller A (2001) Polyoxometalate chemistry: from topology via self-assembly to applications. Springer, Dordrecht
28. Long DL, Tsunashima R, Cronin L (2010) Polyoxometalates: building blocks for functional nanoscale systems. Angew Chem Int Ed 49:1736–1758
29. Seko A, Yamase T, Yamashita KJ (2009) Polyoxometalates as effective inhibitors for sialyl-and sulfotransferases. J Inorg Biochem 103:1061–1066
30. Alhanash A, Kozhevnikova EF, Kozhevnikov IV (2008) Hydrogenolysis of glycerol to propanediol over Ru: polyoxometalate bifunctional catalyst. Catal Lett 120:307–311
31. Neumann R (1998) Polyoxometalate complexes in organic oxidation chemistry. Progr Inorg Chem 47:317–370
32. Zoladek S, Rutkowska IA, Kulesza PJ (2011) Enhancement of activity of platinum towards oxidation of ethanol by supporting on titanium dioxide containing phosphomolybdate-modified gold nanoparticles. Appl Surf Sci 257:8205–8210
33. Triantis T, Troupis A, Gkika E, Alexakos G, Boukos N, Papaconstantinou E, Hiskia A (2009) Photocatalytic synthesis of Se nanoparticles using polyoxometalates. Catal Today 144:2–6
34. D'Souza L, Noeske M, Richards RM, Kortz U (2013) Polyoxotungstate stabilized palladium, gold, and silver nanoclusters: a study of cluster stability, catalysis, and effects of the stabilizing anions. J Colloid Interface Sci 394:157–165
35. Charron G, Giusti A, Mazerat S, Mialane P, Gloter A, Miserque F, Keita B, Nadjo L, Filoramo A, Riviere E, Wernsdorfer W, Huc V, Bourgoin JP, Mallah T (2010) Assembly of a magnetic polyoxometalate on SWNTs. Nanoscale 2:139–144
36. Ma Z, Liu Q, Cui ZM, Bian SW, Song WG (2008) Parallel array of Pt/polyoxometalates composite nanotubes with stepwise inside diameter control and its application in catalysis. J Phys Chem C 112:8875–8880
37. Huang MH, Bi LH, Shen Y, Liu BF, Dong SJ (2004) Nanocomposite multilayer film of Preyssler-type polyoxometalates with fine tunable electrocatalytic activities. J Phys Chem B 112:9780–9786
38. Sun ZX, Xu L, Guo WH, Xu BB, Liu SP, Li FY (2010) Enhanced photoelectrochemical performance of nanocomposite film fabricated by self-assembly of titanium dioxide and polyoxometalates. J Phys Chem C 114:5211–5216
39. Li CX, O'Halloran KP, Ma HY, Shi SL (2009) Multifunctional multilayer films containing polyoxometalates and bismuth oxide nanoparticles. J Phys Chem B 113:8043–8048
40. Kim J, Lee L, Niece BK, Wang JX, Gewirth AA (2004) Formation of ordered multilayers from polyoxometalates and silver on electrode surfaces. J Phys Chem B 108:7927–7933
41. Lin Y, Finke RG (1994) Novel polyoxoanion- and Bu4 N + -stabilized, isolable, and redissolvable, 20-30-.ANG. Ir300-900 nanoclusters: the kinetically controlled synthesis, characterization, and mechanism of formation of organic solvent-soluble, reproducible size, and reproducible catalytic activity metal nanoclusters. J Am Chem Soc 116:8335–8373
42. Aiken JD, Finke RG (1999) Polyoxoanion- and tetrabutylammonium-stabilized Rh(0)(n) nanoclusters: unprecedented nanocluster catalytic lifetime in solution. J Am Chem Soc 121:8803–8810
43. Özkar S, Finke RG (2002) Nanocluster formation and stabilization fundamental studies: ranking commonly employed anionic stabilizers via the development, then application, of five comparative criteria. J Am Chem Soc 124:5796–5810
44. Finke RG, Özkar S (2004) Molecular insights for how preferred oxoanions bind to and stabilize transition-metal nanoclusters: a tridentate, C_3 symmetry, lattice size-matching binding model. Coord Chem Rev 248:135–146
45. Mayer C, Neveu S, Cabuil V (2002) A nanoscale hybrid system based on gold nanoparticles and heteropolyanions. Angew Chem Int Ed 41:501–503
46. Keita B, Liu T, Nadjo L (2009) Synthesis of remarkably stabilized metal nanostructures using polyoxometalates. J Mater Chem 19:19–33
47. Hegde S, Joshi S, Mukherjee T, Kapoor S (2013) Formation of gold nanoparticles via a thiol functionalized polyoxometalate. Mater Sci Eng C 33:2332–2337
48. Keita B, Biboum RN, Mbomekalle IM, Floquet S, Simonnet-Jegat C, Cadot E, Miserque F, Berthet P, Nadjo L (2008) One-

step synthesis and stabilization of gold nanoparticles in water with the simple oxothiometalate $Na_2[Mo_3(\mu_3\text{-}S)(\mu\text{-}S)_3(Hnta)_3]$. J Mater Chem 18:3196–3199
49. Keita B, Zhang G, Dolbecq A, Mialane P, Sécheresse F, Miserque F, Nadjo L (2007) MoV − MoVImixed valence polyoxometalates for facile synthesis of stabilized metal nanoparticles: electrocatalytic oxidation of alcohols. J Phys Chem C 111:8145–8148
50. Keita B, Mbomekalle IM, Nadjo L, Haut C (2004) Tuning the formal potentials of new V^{IV}-substituted Dawson-type polyoxometalates for facile synthesis of metal nanoparticles. Electrochem Commun 6:978–983
51. Keita B, Zhang G, Dolbecq A, Mialane P, Sécheresse F, Miserque F, Nadjo L (2007) Green chemistry-type one-step synthesis of silver nanostructures based on Mo^{V}–Mo^{VI} mixed-valence polyoxometalates. Chem Mater 19:5821–5823
52. Sokolov MN, Fedin VP, Sykes AG (2003) Chalcogenide-containing metal clusters. Compr Coord Chem 3:761–824
53. Bao YY, Bi LH, Wu LX (2011) One-step synthesis and stabilization of gold nanoparticles and multilayer film assembly. J Solid State Chem 184:546–556
54. Liu R, Li S, Yu X, Zhang G, Zhang S, Yao J, Keita B, Nadjo L, Zhi L (2012) Facile synthesis of Au-nanoparticle/polyoxometalate/graphene tricomponent nanohybrids: an enzyme-free electrochemical biosensor for hydrogen peroxide. Small 8:1398–1406
55. Ayati A, Ahmadpour A, Bamoharram FF, Heravi MM, Sillanpää M (2012) Rate redox-controlled green photosynthesis of gold nanoparticles using H3 + xPMo12 − xVxO40. Gold Bull 45:145–151
56. Xu M, Liu C, Xu Y, Li W, Wu L (2009) Incorporation of metal nanoparticles into $H_3PMo_{12}O_{40}$ hybrid Langmuir-Blodgett film through in situ reduction. Colloids Surf A 333:46–52
57. Zhang GJ, Keita B, Biboum RN, Miserque F, Berthet P, Dolbecq A, Mialane P, Catala L, Nadjo L (2009) Synthesis of various crystalline gold nanostructures in water: the polyoxometalate β-$[H_4PMo_{12}O_{40}]^{3-}$ as the reducing and stabilizing agent. J Mater Chem 19:8639–8644
58. Mitchell SG, de la Fuente JM (2012) The synergistic behavior of polyoxometalates and metal nanoparticles: from synthetic approaches to functional nanohybrid materials. J Mater Chem 22:18091–18100
59. Alotaibi MA, Kozhevnikova EF, Kozhevnikov IV (2012) Deoxygenation of propionic acid on heteropoly acid and bifunctional metal-loaded heteropoly acid catalysts: reaction pathways and turnover rates. Appl Catal A 447–448:32–40
60. Seemann KM, Bauer A, Kindervater J, Meyer M, Besson C, Luysberg M, Durkin P, Pyckhout-Hintzen W, Budisa N, Georgii R, Schneider CM, Kogerler P (2013) Polyoxometalate-stabilized, water dispersible Fe_2Pt magnetic nanoparticles. Nanoscale 5:2511–2519
61. Villanneau R, Roucoux A, Beaunier P, Brourief D, Proustab A (2014) Simple procedure for vacant POM-stabilized palladium (0) nanoparticles in water: structural and dispersive effects of lacunary polyoxometalates. RSC Adv 4:26491–26498
62. Li HL, Yang Y, Wang YZ, Li W, Bi LH, Wu LX (2010) In situ fabrication of flower-like gold nanoparticles in surfactant-polyoxometalate-hybrid spherical assemblies. Chem Commun 46:3750–3752
63. Friedrich H, Frederik PM, de With G, Sommerdijk NAJM (2010) Imaging of self-assembled structures: interpretation of TEM and Cryo-TEM images. Angew Chem Int Ed 49: 7850–7858
64. Wang Y, Neyman A, Arkhangelsky E, Gitis V, Meshi L, Weinstock IA (2009) Self-assembly and structure of directly imaged inorganic-anion monolayers on a gold nanoparticle. J Am Chem Soc 131:17412–17422
65. Geletii YV, Hill CL, Atalla RH, Weinstock IA (2006) Reduction of O_2 to superoxide anion (O^{2-}) in water by heteropolytungstate cluster-anion. J Am Chem Soc 128:17033–17042
66. Wang Y, Zeiri O, Gitis V, Neyman A, Weinstock IA (2010) Reversible binding of an inorganic cluster-anion to the surface of a gold nanoparticle. Inorg Chim Acta 363:4416–4420
67. Wang Y, Weinstock IA (2010) Cation mediated self-assembly of inorganic cluster anion building blocks. Dalton Trans 39:6143–6152
68. Wang Y, Zeiri O, Sharet S, Weinstock IA (2012) Role of the alkali-metal cation size in the self-assembly of polyoxometalate-monolayer shells on gold nanoparticles. Inorg Chem 51:7436–7438
69. Wang Y, Zeiri O, Neyman A, Stellacci F, Weinstock IA (2012) Nucleation and island growth of alkanethiolate ligand domains on gold nanoparticles. ACS Nano 6:629–640
70. Graham CR, Ott LS, Finke RG (2009) Ranking the lacunary $(Bu_4N)_9\{H[\alpha_2\text{-}P_2W_{17}O_{61}]\}$ polyoxometalate's stabilizing ability for $Ir(0)_n$ nanocluster formation and stabilization using the five-criteria method plus necessary control experiments. Langmuir 25:1327–1336
71. Lica G, Browne K, Tong Y (2006) Interactions between Keggin-type lacunary polyoxometalates and Ag nanoparticles: a surface-enhanced raman scattering spectroscopic investigation. J Cluster Sci 17:349–359
72. Liu T, Langston MLK, Li D, Pigga JM, Pichon C, Todea AM, Müller A (2011) Self-recognition among different polyprotic macroions during assembly processes in dilute solution. Science 331:1590–1592
73. Aparicio-Angles X, Clotet A, Bo C, Poblet JM (2011) Towards the computational modelling of polyoxoanions on metal surfaces: IR spectrum characterisation of $[SiW_{12}O_{40}]^{4-}$ on Ag(111). Phys Chem Chem Phys 13:15143–15147
74. Antonio MR, Nyman M, Anderson TM (2009) Direct observation of contact ion-pair formation in aqueous solution. Angew Chem Int Ed 48:6136–6140
75. Niu C, Wu Y, Wang Z, Li Z, Li R (2009) Synthesis and shapes of gold nanoparticles by using transition metal monosubstituted heteropolyanions as photocatalysts and stabilizers. Front Chem China 4:44–47
76. Shankar SS, Rai A, Ahmad A, Sastry M (2005) Controlling the optical properties of lemongrass extract synthesized gold nanotriangles and potential application in infrared-absorbing optical coatings. Chem Mater 17:566–572
77. Li SW, Yu XL, Zhang GJ, Ma Y, Yao JN, Keita B, Nadjo L, Zhao H (2011) Green chemical decoration of multiwalled carbon nanotubes with polyoxometalate-encapsulated gold nanoparticles: visible light photocatalytic activities. J Mater Chem 21:2282–2287
78. Bamoharram FF, Ahmadpour A, Heravi MM, Ayati A, Rashidi H, Tanhaei B (2012) Recent advances in application of polyoxometalates for the synthesis of nanoparticles. Synth React Inorg Chem 42:209–230
79. Ahmadpour A, Bamoharrem FF, Heravi MM, Rashidi H (2011) Photocatalytic synthesis of gold nanoparticles using Preyssler acid and their photocatalytic activity. Chin J Catal 32:978–982
80. Ayati A, Ahmadpour A, Bamoharram FF, Heravi MM (2012) A green and simple route for the controlled-size synthesis of gold nanoparticles using Preyssler heteropolyacid. Synth React Inorg Me 42:1309–1314
81. Bamoharram FF, Heravi MM, Meraji M (2009) Synthesis of silver nanoparticles in the presence of a green heteropolyacid, $H_{14}[NaP_5W_{30}O_{110}]$, and their catalytic activity for photodegradation

of methylene blue and methyl orange. Int J Green Nanotechnol 1:26–31
82. Bamoharram FF (2011) Role of polyoxometalates as green compounds in recent developments of nanoscience. Synth React Inorg Me 41(8):893–922
83. Ayati A, Ahmadpour A, Bamoharram FF, Heravi MM, Rashidi H, Tanhaei B (2011) Application of a new photocatalyst in the preparation of silver nanoparticles and investigating their photocatalytic activity. J Nanostruct Chem 2(1):15–22
84. Ayati A, Ahmadpoura A, Bamoharramb FF, Heravic MM, Tanhaeia B, Sillanpääb M (2012) Facile green synthesis of gold nanorods. International Congress of Chemical Engineering, Sevilla
85. Puddephatt RJ (1978) Compounds with gold-metal bonds. In: Clark RJH (ed) The chemistry of gold. Elsevier, Amsterdam
86. Singh A, Sharp PR (2005) Palladium–gold oxo complexes. Dalton Trans 12:2080–2081
87. Cao R, Anderson TM, Piccoli PMB, Schultz AJ, Koetzle TF, Geletii YV, Slonikina E, Hedman B, Hodgson KO, Hardcastle KI, Fang X, Kirk ML, Knottenbelt S, Kogerler P, Musaev DG, Morokuma K, Takahashi M, Hill CL (2007) Terminal gold-oxo complexes. J Am Chem Soc 129:11118–11133
88. Bagno A, Bini R (2010) NMR spectra of terminal oxo gold and platinum complexes: relativistic DFT predictions. Angew Chem 122:1101–1104
89. Corma A, Dominguez I, Domenech A, Fornes V, Gomez-Garcia CJ, Rodenas T, Sabater MJ (2009) Enantioselective epoxidation of olefins with molecular oxygen catalyzed by gold(III): a dual pathway for oxygen transfer. J Catal 265:238–244
90. Izarova NV, Vankova N, Heine T, Biboum RN, Keita B, Nadjo L, Kortz U (2010) Polyoxometalates made of gold: the polyoxoaurate [(Au4As4O20)-As-III-O-V](8-). Angew Chem Int Ed 49:1886–1889
91. Tebandeke E, Coman C, Guillois K, Canning G, Ataman E, Knudsen J, Wallenberg LR, Ssekaalo H, Schnadtb J, Wendt OF (2014) Epoxidation of olefins with molecular oxygen as the oxidant using gold catalysts supported on polyoxometalates. Green Chem 16:1586–1593
92. An D, Ye A, Deng W, Zhang Q, Wang Y (2012) Selective conversion of cellobiose and cellulose into gluconic acid in water in the presence of oxygen, catalyzed by polyoxometalate-supported gold nanoparticles. Chem Eur J 18:2938–2947
93. Biboum RN, Keita B, Franger S, Njiki CPN, Zhang G, Zhang J, Liu T, Mbomekalle I, Nadjo L (2010) Pd^0@polyoxometalate nanostructures as green electrocatalysts: illustrative example of hydrogen production. Materials 3:741–754
94. Wang Y, Weinstock IA (2012) Polyoxometalate-decorated nanoparticles. Chem Soc Rev 41:7479–7496
95. Babakhanian A, Kaki S, Ahmadi M, Ehzari H, Pashabadi A (2014) Development of alpha-polyoxometalate-polypyrrole-Au nanoparticles modified sensor applied for detection of folic acid. Biosens Bioelectron 60:185–190
96. Li S, Maa H, O'Halloran KP, Pang H, Hongrui J, Zhou C (2013) Enhancing characteristics of a composite film by combination of vanadium-substituted molybdophosphate and platinum nanoparticles for an electrochemical sensor. Electro Chim Acta 108:717–726
97. Hou W, Cronin SB (2013) A review of surface plasmon resonance-enhanced photocatalysis. Adv Funct Mater 23:1612–1619
98. Solarska R, Bienkowski K, Zoladek S, Majcher A, Stefaniuk T, Kulesza PJ, Augustynski J (2014) Enhanced water splitting at thin film tungsten trioxide photoanodes bearing plasmonic gold–polyoxometalate particles. Angew Chem Int Ed 53: 14196–14200
99. Vazylyev M, Sloboda-Rozner D, Haimov A, Maayan G, Neumann R (2005) Strategies for oxidation catalyzed by polyoxometalates at the interface of homogeneous and heterogeneous catalysis. Top Catal 34:93–99
100. Zhang M, Weinstock IA, Wang Y (2014) Electrocatalysis by polyoxometalate-protected gold nanoparticles. J Clust Sci 25:771–779
101. Ernst AZ, Zoladek S, Wiaderek K, Coxb JA, Zurowskaa AK, Miecznikowski K, Kulesza PJ (2008) Network films of conducting polymer-linked polyoxometalate-modified gold nanoparticles: preparation and electrochemical characterization. Electrochimi Acta 53:3924–3931
102. Barczuk PJ, Lewera A, Miecznikowski K, Zurowski A, Kulesza PJ (2010) Enhancement of catalytic activity of platinum-based nanoparticles towards electrooxidation of ethanol through interfacial modification with heteropolymolybdates. J Power Sour 195:2507–2513
103. Zoladek S, Rutkowskaa IA, Skorupska K, Palys B, Kuleszaa PJ (2011) Fabrication of polyoxometallate-modified gold nanoparticles and their utilization as supports for dispersed platinum in electrocatalysis. Electrochim Acta 56:10744–10750
104. Weinberg HS, Delcomyn CA, Unnan V (2003) Bromate in chlorinated drinking waters: occurrence and implications for future regulation. Environ Sci Technol 37:3104–3110
105. Ernst AZ, Sun L, Wiaderek K, Kolary A, Zoladek S, Kulesza PJ, Cox JA (2007) Synthesis of polyoxometalate-protected gold nanoparticles by a ligand-exchange method: application to the electrocatalytic reduction of bromate. Electroanal 19:2103–2109
106. Karnicka K, Chojak M, Miecznikowski K, Skunik M, Baranowska B, Kolary A, Piranska A, Palys B, Adamczyk L, Kulesza PJ (2005) Polyoxometalates as inorganic templates for electrocatalytic network films of ultra-thin conducting polymers and platinum nanoparticles. Bioelectrochem 66:79–87
107. Turyan I, Mandler D (1998) Two-dimensional polyaniline thin film electrodeposited on a self-assembled monolayer. J Am Chem Soc 120:10733–10742
108. Miyazaki A, Nakano Y (2000) Morphology of platinum nanoparticles protected by poly(*N*-isopropylacrylamide). Langmuir 16:7109–7111
109. Ahmadi TS, Wang ZL, Green TC, Henglein A, El-Sayed MA (1996) Shape-controlled synthesis of colloidal platinum nanoparticles. Science 272:1924–1925
110. Wiaderek KM, Cox JA (2011) Preparation and electrocatalytic application of composites containing gold nanoparticles protected with rhodium-substituted polyoxometalates. Electrochimi Acta 56:3537–3542
111. Kriz K, Anderlund M, Kriz D (2001) Real-time detection of l-ascorbic acid and hydrogen peroxide in crude food samples employing a reversed sequential differential measuring technique of the SIRE-technology based biosensor. Biosens Bioelectron 16:363–369
112. Baskar S, Chang JL, Zen JM (2012) Simultaneous detection of NADH and H_2O_2 using flow injection analysis based on a bifunctional poly(thionine)-modified electrode. Biosens Bioelectron 33:95–99
113. Teymourian H, Salimi A, Hallaj R (2012) Low potential detection of NADH based on Fe_3O_4 nanoparticles/multiwalled carbon nanotubes composite: fabrication of integrated dehydrogenase-based lactate biosensor. Biosens Bioelectron 33:60–68
114. Won YH, Aboagye D, Jang HS, Jitianu A, Stanciu LA (2010) Core/shell nanoparticles as hybrid platforms for the fabrication of a hydrogen peroxide biosensor. J Mater Chem 20:5030–5034
115. Lin KC, Tsai TH, Chen SM (2010) Performing enzyme-free H_2O_2 biosensor and simultaneous determination for AA, DA, and UA by MWCNT–PEDOT film. Biosens Bioelectron 26:608–614
116. Claussen JC, Franklin AD, Haque AU, Porterfield DM, Fisher TS (2009) Electrochemical biosensor of nanocube-augmented carbon nanotube networks. ACS Nano 3:37–44

117. Zhang Y, Bo X, Nsabimana A, Munyentwali A, Han C, Li M, Guo L (2015) Green and facile synthesis of an Au nanoparticles@polyoxometalate/ordered mesoporous carbon tri-component nanocomposite and its electrochemical applications. Biosens Bioelectron 66:191–197
118. Li S, Yu X, Zhang G, Ma Y, Yao J, de Oliveira P (2011) Green synthesis of a Pt nanoparticle/polyoxometalate/carbon nanotube tri-component hybrid and its activity in the electrocatalysis of methanol oxidation. Carbon 49:1906–1911
119. Wang Y, Zhang S, Du D, Shao YY, Li ZH, Wang J, Engelhard MH, Li JH, Lin YH (2011) Self assembly of acetylcholinesterase on a gold nanoparticles–graphene nanosheet hybrid for organophosphate pesticide detection using polyelectrolyte as a linker. J Mater Chem 21:5319–5325
120. Yang MH, Choi BG, Park H, Park TJ, Hong WH, Lee SY (2011) Directed self-assembly of gold nanoparticles on graphene-ionic liquid hybrid for enhancing electrocatalytic activity. Electroanal 23:850–857
121. Liu RJ, Li SW, Yu XL, Zhang GJ, Ma Y, Yao JN, Keita B, Nadjo L (2011) Polyoxometalate-assisted galvanic replacement synthesis of silver hierarchical dendritic structures. Cryst Growth Des 11:3424–3431
122. Rhule JT, Hill CL, Judd DA, Schinazi RF (1998) Polyoxometalates in medicine. Chem Rev 98:327–357
123. Yamase T (2005) Anti-tumor, -viral, and -bacterial activities of polyoxometalates for realizing an inorganic drug. J Mater Chem 15:4773–4782
124. Hasenknopf B (2005) Polyoxometalates: introduction to a class of inorganic compounds and their biomedical applications. Front Biosci 10:275–287
125. Daima HK, Selvakannan PR, Shukla R, Bhargava SK, Bansal V (2013) Fine-tuning the antimicrobial profile of biocompatible gold nanoparticles by sequential surface functionalization using polyoxometalates and lysine. PLoS One 8:1–14